HHS Public Access

Author manuscript

Oncogene. Author manuscript; available in PMC 2016 May 18.

Published in final edited form as:

Oncogene. 2015 November 26; 34(48): 5879–5889. doi:10.1038/onc.2015.44.

Cell growth density modulates cancer cell vascular invasion via Hippo pathway activity and CXCR2 signaling

Ghada M Sharif, **Marcel O Schmidt**, **Chunling Yi**, **Zhangzhi Hu**, **Bassem R. Haddad**, **Eric Glasgow**, **Anna T Riegel**, and **Anton Wellstein***

Lombardi Cancer Center, Georgetown University, Washington, DC 20007, USA

Abstract

Metastasis of cancer cells involves multiple steps, including their dissociation from the primary tumor and invasion through the endothelial cell barrier to enter the circulation and finding their way to distant organ sites where they extravasate and establish metastatic lesions. Deficient contact inhibition is a hallmark of invasive cancer cells, yet surprisingly the vascular invasiveness of commonly studied cancer cell lines is regulated by the density at which cells are propagated in culture. Cells grown at high density were less effective at invading an endothelial monolayer than cells grown at low density. This phenotypic difference was also observed in a zebrafish model of vascular invasion of cancer cells after injection into the yolk sac and extravasation of cancer cells into tissues from the vasculature. The vascular invasive phenotypes were reversible. A kinome-wide RNAi screen was used to identify drivers of vascular invasion by panning shRNA library transduced non-invasive cancer cell populations on endothelial monolayers. The selection of invasive subpopulations showed enrichment of shRNAs targeting the LATS1 (large tumor suppressor 1) kinase that inhibits the activity of the transcriptional coactivator YAP in the Hippo pathway. Depletion of LATS1 from non-invasive cancer cells restored the invasive phenotype. Complementary to this, inhibition or depletion of YAP inhibited invasion in vitro and in vivo. The vascular invasive phenotype was associated with a YAP-dependent up-regulation of the cytokines IL6, IL8, and CXCL1, 2, and 3. Antibody blockade of cytokine receptors inhibited invasion and confirmed that they are rate-limiting drivers that promote cancer cell vascular invasiveness and could provide therapeutic targets.

Introduction

One hallmark of cancer is the capacity of malignant cells to enter the circulation by interrupting the vascular endothelial barrier at the primary site (=invasion) and transverse the vasculature at a distant organ site to initiate a metastatic seed (=extravasation). Metastatic

*Corresponding author. Tel: +1 (202) 687-3672; ; Email: wellstea@georgetown.edu

Author contributions

GMS and AW designed the research and wrote the paper. GMS, MOS, and EG performed the research. All authors discussed the results and commented on the manuscript.

Conflict of interest

The authors declare that they have no conflict of interest.

seeding can start at the earliest phases of malignancies and is the major cause of later disease recurrence [1, 2]. Cancer cells acquire the ability to metastasize through cell-autonomous mechanisms or recruit tissue-infiltrating monocytes to support this process [3–5]. Also, subpopulations of cancer cells may alter the overall invasiveness of a tumor even when present as a small fraction [6]. We sought to understand underlying mechanisms and identify the driver pathways of cancer cell vascular invasion. Contact inhibition ensures that epithelial cells will stop proliferation once they have reached confluence. In contrast, cancer cells continue proliferating in spite of interactions with neighboring cells, are typically refractory to contact inhibition and often display anchorage-independent growth in suspension. The gain of anchorage-independent growth, the loss of anoikis in response to detachment as well as the loss of contact inhibition are hallmarks of cancer cells [7]. This also suggests that oncogenic alterations can uncouple contact inhibition mechanisms from cell growth and survival pathway signals [8].

Much to our surprise, we found that altering the density at which the cancer cells are propagated enhanced or reduced the vascular invasiveness of commonly studied, highly aggressive cancer cell lines. To identify possible drivers along the pathways that control this cell contact-dependent behavior of cancer cell, we performed an unbiased RNAi screen. In this screen human kinome-wide shRNA transduced, pooled cancer cells were rendered non-invasive by growth at high density and then were selected for invasive subpopulations generated by knockdown biologically significant kinases. We identied the LATS1 kinase in the Hippo pathway as a hub that controls vascular invasiveness of cancer cells grown at different densities. The LATS “large tumor suppressor” gene had been identified in a drosophila mosaic screen and its mammalian tumor suppressive function established thereafter [9, 10]. The LATS kinase cascade controls the activity of transcriptional coactivators YAP and the related TAZ. An ever increasing number of upstream extracellular signals have been identified that are integrated via YAP/TAZ transcriptional regulation during organ growth and in maintaining tissue homeostasis [11–13]. The physiologic function of Hippo pathway activity is apparent during the earliest stages of development when pathway activity impacts cell fate decisions in the inner cell mass relative to the surface trophoectoderm that forms the placenta in mammals. The intricate crosstalk during embryonic inner mass development relies on signaling molecules that control cell polarity and cell-cell crosstalk and switches to distinct organ specific pathways that may be impacted during malignant transformation (reviewed in [13–15]). Invasive cancers frequently develop after YAP-induced organ overgrowth suggesting a fundamental role of pathologic organ size control mechanism in malignancies [16–18]. Also, YAP has been found upregulated in different types of human cancers, was shown to correlate with poor disease outcome and is considered an attractive therapeutic target [19, 20]. YAP transcriptional activity was more recently linked to metastasis in melanoma, lung and breast cancer [21–23], was shown to be rate limiting for malignant progression of Kras-driven pancreatic cancer [24] and expression of YAP appears to be sufficient to overcome the loss of Kras signaling in Kras dependent cancers [25]. Here we report Hippo pathway signalling mechanisms that control vascular invasiveness of cancer cell lines.

Results

Cancer cell growth density impacts their vascular invasion

To identify the drivers of cancer cell vascular invasion, we used a co-culture system that records in real-time the disruption and invasion of an intact endothelial monolayer by cancer cells. The process can be monitored by electric cell impedance sensing (ECIS), which provides a continuous readout of the status of the endothelial monolayer (Figure 1a and 1b). When maintained at low cell density, triple-negative human MDA-MB-231 breast cancer cells that are widely used for modelling cellular invasion showed an easily discernible endothelial monolayer invasive phenotype (ECIS assay; Figure 1b and 1c). This was also observed with derivative MDA-MB-231 cell lines selected by the Massagué laboratory to metastasize to the brain, bone or lung [26–28] (Figure 1d). Surprisingly, when these cell lines were grown at high density for a short time, their invasiveness was significantly reduced to levels barely above the background (Figure 1c, d). This non-invasive phenotype was not caused by different rates of cell proliferation or apoptosis (Supplementary Figure S1A and S1B) and was reversed by switching the cells to the low-density growth condition. Cell density was also found to influence the invasiveness of PC3 (prostate cancer), U87-MG (glioblastoma), and E0771 (mouse mammary carcinoma) cells (Figure 1d). Cell density did not, however, influence the invasiveness of Colo357 pancreatic cancer cells, which attach to each other in cell culture to form 3D organoid structures at low and at high cell density. Thus, the in vitro invasiveness of several established and widely used cancer cell lines into endothelial monolayers is highly dependent on cell growth density.

To evaluate whether these distinct in vitro phenotypes would be recapitulated in vivo, we evaluated cancer cell trafficking in zebrafish models [29]. Cancer cells grown at different densities were labelled with colored tracers, injected into transparent zebrafish embryos, and their subsequent trafficking into the vasculature and extravasation into target tissues were visualized over several days. First, we tested the ability of MDA-MB-231 cells to invade the circulation. Identical numbers of MDA-MB-231 cells grown at high or low densities were labelled with red or green dyes respectively and were simultaneously injected into zebrafish yolk sacs (Figure 2a and 2b). While MDA-MB-231 cells grown at low density (green) entered the circulation and were visible inside the tail vasculature, MDA-MB-231 cells grown at high density (red) rarely entered the vasculature (Figure 2c and 2d). Also, MDA-MB-231 cells grown at either high or low density were labelled with the same colored tracer and injected separately into the yolk sacs of zebrafish. Similarly, MDA-MB-231 cells grown at low density were able to extravasate into the vasculature more readily than cells grown at high density (Supplementary Figure S1C). Thus, the effect of growth density on endothelial monolayer invasiveness of MDA-MB-231 cells was also apparent during invasion into the vasculature of an intact organism.

Next, extravasation and peripheral tissue invasion of MDA-MB-231 cells was monitored in transgenic zebrafish expressing green reef coral fluorescent protein (GRCFP) in the vascular endothelia under the control of a VEGFR2 promoter [Tg(kdrl:GRCFP)zn1; [30]]. MDA-MB-231 cells labelled with red fluorescent dye were injected directly into the circulation of these fish, and cells that exited the blood vessels and invaded the surrounding tissues were

counted (Figure 2e and 2f). The low density MDA-MB-231 cells extravasated at a significantly higher rate than the high density cells (Figure 2g), similar to the increased intravasation from the yolk sac injection shown above (see Figure 2d). Also, in a mouse model of experimental metastasis confluent MDA-MB-231 cells colonized the lungs significantly less efficiently than cells grown at low density (Supplementary Figure S1D) consistent with a distinct vascular invasive phenotype.

LATS1-YAP activity is a rate-limiting switch for cancer cells vascular invasion

To identify drivers that modulate vascular invasiveness in response to cell density, we carried out an RNAi screen with MDA-MB-231 cells transduced with a human kinome-targeted shRNA library (Figure 3a). Pooled cells were grown to high density to suppress their attachment to endothelial monolayers (Supplementary Figure S1E) and invasive phenotype (see Figure 1c). A subpopulation of shRNA-transduced cells that invade endothelial monolayers was selected by panning on endothelial monolayers. The subpopulation was harvested and expanded to high density growth for consecutive rounds of further selection. Analysis of shRNA barcodes expressed in the selected invasive subpopulation showed a 16.6-fold to 57.3-fold enrichment of three different shRNAs targeting LATS1 (large tumor suppressor, homologue 1; Supplementary Table 2), a serine/threonine kinase that phosphorylates and represses YAP activity by preventing its nuclear translocation (Figure 3b) [11]. To confirm LATS1 involvement in endothelial attachment and invasion, MDA-MB-231 cells with LATS1 knockdown were grown at low or high density. After LATS1 depletion transendothelial invasion of high density cells was as effective as the invasive population that had been grown at low density. Furthermore, LATS1 depletion did not impact the invasive phenotype of cells grown at low density (Figure 3c, d).

YAP activity and nuclear translocation is mediated by phosphorylation at serine-127 by the LATS kinase [11] and we thus analyzed MDA-MB-231, E0771 and Colo357 cells for the status of YAP phosphorylation and subcellular localization during growth at different cell densities. As shown in Supplementary Figure S2A and S2B, the levels of pYAP(S127) were reduced in MDA-MB-231 and E0771 cells but not in Colo357 cells grown at low density. YAP cytoplasmic sequestration was also evident in MDA-MB-231 and E0771 cells, but not in Colo357 cells when grown at high density (Supplementary Figure S2C). Corresponding to decreased phosphorylation and increased nuclear localization of YAP in low density MDA-MB-231 cells, we found that the YAP target genes CTGF and CYR61 were upregulated compared to cells grown at high density (Supplementary Figure S2D). To further examine the cell density-dependent response of YAP, MDA-MB-231 cells, grown at low or high density, were dissociated to a single cell suspension and cultured at high or low cell density, respectively. YAP localization and phosphorylation status were monitored over time as indicators of altered Hippo pathway activity. The high density cells retained some YAP cytoplasmic localization and phosphorylation until the 48 hour time point after switching to low density. Vice versa, the low density cells lost YAP nuclear localization and gained YAP phosphorylation when plated at high density around the 24 hour time point (Supplementary Figure S3).

To further evaluate the contribution of YAP activity to endothelial invasion, we treated MDA-MB-231 and E0771 cells with verteporfin (VP), a recently identified small-molecule inhibitor of YAP activity [31] and found that it inhibited CTGF and CYR61 expression (Supplementary Figure S2E and S2F). Also, endothelial invasion and transwell migration of low density MDA-MB-231 and E0771 cells were inhibited by VP in a dose-dependent fashion (Figure 3e to 3i). Furthermore, YAP knockdown in MDA-MB-231 and E0771 cells reduced invasion and migration when cells were grown at low density (Supplementary Figure 4A to D). These data link YAP activity to endothelial invasiveness of cancer cells in vitro in response to altered cell density.

To assess the role of YAP for vascular invasion in vivo, low-density MDA-MB-231 cells were treated with VP before injection into the zebrafish circulation. Vehicle-treated MDA-MB-231 cells extravasated more efficiently than the VP-treated cells (Figure 4a and 4d). Similarly, YAP knockdown in E0771 cells significantly reduced the extravasation of these cells from the zebrafish vasculature (Figure 4b, 4c and 4e). Finally, E0771 cells carrying control or YAP shRNAs were injected into the tail veins of nude mice to follow the ability of these cells to colonize the lungs. Histological examination of lungs (Figure 4f) and quantitative PCR analysis for the puromycin resistance gene (present in cells carrying the shRNAs) showed that YAP knockdown significantly reduced the ability of E0771 cells to colonize the lungs (Figure 4g). Liver tissues served as a negative control and will capture potential signals from cancer cells in the circulation.

Lung metastases of E0771 control cells (Figure 4f) displayed a wide range of sizes with the smallest consisting of single cell layers with less than 20 cells surrounding an associated blood vessel. When staining for YAP we noted that in these small metastases almost all cancer cells displayed nuclear location of the YAP protein, whereas larger metastases contained a significantly lower portion of cells with nuclear YAP (~50% of cells; Figure 5a and 5b). On the other hand, the percentage of cancer cells staining positive for PCNA (= proliferating cell nuclear antigen; ~60%) was indistinguishable between small and large metastases or between cells located closer to and more distant from a blood vessel (Figure 5c and 5d). Also, staining of serial sections revealed no correlation between PCNA expression and nuclear YAP. Thus, the nuclear localization of YAP in small metastases was not caused by a higher cell proliferation rate but appears to indicate the more invasive phenotype of cancer cells after their initial extravasation that required the disruption of the local endothelial barrier. This finding also shows the dissociation between proliferative and invasive signaling.

Autocrine and paracrine signaling by cytokines from cancer cells

To further elucidate the downstream mechanisms driving endothelial invasiveness, we compared the gene expression profiles of MDA-MB-231 cells grown at high and low densities. Significant upregulation ($p<0.01$) of cytokines (IL1, 6, and 8; CXCL1, 2, and 3), hematopoietic growth factors (GMCSF=CSF2 and GCSF=CSF3), genes involved in cell adhesion, migration, and metastasis, including CD44 [32, 33] and tenascin C [34] was observed in MDA-MB-231 cells grown at low density (Figure 6a). Comparative genomic hybridization (CGH) analysis of cells kept at low or high growth density ruled out genomic

differences at the loci of differently regulated genes in response to altered growth conditions (Supplementary Figure S5).

The upregulation of cytokines in low density MDA-MB-231 cells correlated with increased phosphorylation of Stat3, an intracellular mediator of cytokine signalling, and NFκB, a downstream mediator of JAK/STAT signalling (Supplementary Figure S2A). Furthermore, MDA-MB-231 cells grown at low density showed up-regulation of vimentin and down-regulation of beta-catenin and E-cadherin (Supplementary Figure S2A), indicative of having acquired more mesenchymal characteristics. Pathway analysis revealed that canonical cytokine signaling and the respective downstream signal transduction modules are the most prominently upregulated pathways in low density MDA-MB-231 cells (Supplementary Figure S6A).

To directly examine YAP regulation of cytokine expression and release from cells, we collected and analyzed cancer-cell conditioned media (CM) from low-density MDA-MB-231 cells treated with vehicle (control) or with the YAP inhibitor VP. As shown in Supplementary Figure S6B and S6C, VP treatment significantly reduced the amount of secreted cytokines that were also found differentially expressed when comparing low density and high density growth MDA-MB-231 cells. This included IL1 alpha and beta; IL8; CXCL1, 2, and 3; GMCSF and GCSF (see Figure 6A). Also, adding exogenous CXCL1 and IL8 enhanced invasion and migration when YAP was knocked down in MDA-MB-231 and E0771 cells (Supplementary Figure S4A, S4E and S4F).

To investigate how these cytokine activities may modulate endothelial function in trans, we harvest conditioned media (CM) from MDA-MB-231 cells grown at low or high cell density and applied them to a disrupted endothelial monolayer in a wound healing assay. In this ECIS based assay, the kinetics of monolayer repair is followed in real-time (Supplementary Figure S7A and S7B). CM from low density MDA-MB-231 cells delayed closure of the wounds in a dose-dependent fashion (Supplementary Figure S7C and S7D), whereas CM from high density cells showed no discernible effect (Supplementary Figure S7B). In composite, this implies a role of factors in conditioned media from low density cells in loosening the endothelial monolayer, preventing tight junction from reforming and maintaining vascular permeability, all of which are important for cancer cell crossing of an endothelial barrier.

CXCR2 is the cognate receptor for CXCL1, 2, 3 and IL8 (=CXCL8) which are differentially expressed in MDA-MB-231 cells grown at low versus high cell density (Figure 6a). Treatment with a CXCR2 blocking antibody inhibited endothelial monolayer invasion and transwell migration by low density MDA-MB-231 cells, reducing their invasiveness to the same level as that of high density MDA-MB-231 cells (Figure 6b and 6c). Also, pre-treatment of an endothelial monolayer with the CXCR2 blocking antibody prior to wounding showed a slightly faster closure of the wound and reverted the delay in wound closure caused by conditioned media from low density cancer cells (Supplementary Figure S7E and S7F). Thus, cytokines released from cancer cells grown at low density will function in a paracrine and in an autocrine fashion to support transendothelial invasion.

Cytokine signaling and vascular invasion

To evalute the impact of CXCR2 pathway activation on cancer cell invasiveness in vivo, low-density MDA-MB-231 cells were pretreated with an anti-CXCR2 antibody prior to injection into the kdr1:GRCFP zebrafish model described above (see Figure 2e). Inspection of 3D images of red labeled cancer cells relative to the vascular network demarkated by endothelial GFP revealed that the homing pattern of anti-CXCR2 pretreated cancer cells was significantly different from that of the untreated cells. In contrast to the controls, the treated cancer cells accumulated in the caudal vein plexus (CVP) (Figure 6d) and preferentially extravasated from the CVP region rather than from intersegmental vessel in the tail of the zebrafish (Figure 6e, Day 1). The tissue invasion patterns of the treated and untreated cells remained significantly different also on the second day of observation, although the difference was less pronounced, possibly because of a diminishing antibody blocking effect. It is noteworthy that the CVP of the zebrafish is analogous to the fetal hematopoietic organ (the liver) in mammals: The CVP is rich in growth factors controlling hematopoietic stem cell differentiation and the expansion of differentiated hematopoietic cell lineages. Also, IL8 and its receptors CXCR1 and CXCR2 are conserved between mammals and zebrafish, and can modulate inflammatory signals [35, 36]. Because MDA-MB-231 cells respond to additional exogenous IL8 with enhanced migration (Figure 6c), we propose that the anti-CXCR2 treatment redirects the cancer cells to the CVP that provides a plethora of local growth factors and cytokines that may help the cancer cells overcome the CXCR2 blockade.

Discussion

Here we report that altering the growth density of widely used cancer cell lines impacts their capacity for endothelial monolayer invasion in vitro and vascular invasion and metastatic seeding in vivo. This phenotypic hallmark of cancer cells [37] was surprisingly malleable by cell culture conditions and is modulated through secreted growth factors that signal via autocrine and paracrine pathways (Figure 7). A kinome-wide RNAi screen identified the tumor suppressor LATS1 upstream of YAP as the rate-limiting kinase that prevents endothelial invasion of cells grown at high density (Figure 3a and 3b). Knockdown of LATS1 in a non-invasive cancer cell population grown at high density rendered these cells as invasive as a population grown at low density (Figure 3c). Complementary to this, the inhibition of YAP in cancer cells kept at low growth density suppressed their invasive phenotype in vitro and in vivo (Figure 3 and 4). The Hippo pathway has been implicated in metastasis [21, 23] and we now show its contribution to cancer cell / endothelial crosstalk and vascular invasion. Cancer cells grown at low density to induce invasiveness upregulated expression of several cytokines in parallel with nuclear translocation of YAP. Inhibition of YAP using the inhibitor Verteporfin reversed this upregulation (Figure 6a, Supplementary Figure S6). The most upregulated cytokines under invasive cell growth conditions use CXCR2 for signaling and we found that antibody blockade of the CXCR2 receptor inhibited the migration, endothelial monolayer invasiveness and extravasation of invasive cancer cells (Figure 6). Thus, we propose that the altered vascular invasive phenotype of cancer cells grown at different densities is mediated through CXCR2 autocrine and paracrine acting cytokines whose expression is controlled by LATS1-YAP.

Control of transcriptional activity of YAP by the upstream kinases MST and LATS is well understood. However, a number of upstream stimuli can be integrated through these molecules and it is likely that these are organ specific. E.g. YAP is dispensable for normal mammary gland development but is required for oncogene-induced mammary gland malignancies [20]. Also, YAP overexpression does not appear to be sufficient for mammary gland transformation [20] but LIFR (leukemia inhibitory factor receptor) was shown to function upstream of YAP and control its oncogenic function. In a whole genome RNAi screen for tumor formation in mice, LIFR was identified as a tumor suppressor in partially transformed, non-tumorigenic mammary epithelial cells. Complementary to this, restoring LIFR expression reduced YAP activity and inhibited metastasis in breast cancer cells [3839]. In contrast to the mammary gland, YAP is required for proper function of the liver and activated YAP will lead to reversible hepatomegaly and to liver cancer [16]. On the other hand we found recently that duct epithelial YAP expression is dispensable for pancreatic development as well as pancreatic endocrine and exocrine function [24]. However, malignant progression to invasive pancreatic ductal carcinoma due to mutant KRAS and p53 depends on the expression of ductal YAP and a set of YAP dependent paracrine acting growth factors and enzymes [24]. It does appear that distinct upstream stimuli may utilize the Hippo pathway for their respective cell type or organ specific activities.

Cytokine expression has been implicated in more aggressive cancer phenotypes based on clinical samples and in mechanistic studies with cultured cells or animal models. Cytokines were found at higher levels in metastases when compared with biopsies of primary tumors. Furthermore, high levels of cytokines were associated with a shorter relapse-free patient survival suggesting their impact on the aggressiveness of the particular cancer [40]. Cancers can overexpress CXCL1 & 2 [41], IL6 [42], IL8 [5] or activate CXCR2/R4 pathways due to a loss of TGF-beta signaling and thus attract mesenchymal cells that respond to these cytokines [43]. This influx of inflammatory cells can provide additional cytokine activity that enhances cancer cell survival or expansion of the stem cell population [43, 44] and leads to poor disease outcome and/or treatment resistance [41]. Furthermore, cancer cells in the circulation can be attracted into emerging metastases by their cytokine expression gradient, and expand the lesion through selfseeding of cancer cells [45].

Epithelial-mesenchymal transition (EMT) signatures were found associated with, and controlled by increased expression of IL6 [42] or IL8 [46] and were observed here under low cell growth density conditions (Supplementary Figure S2A). In our study E-cadherin is upregulated by high density growth of MDA-MB-231 cells and coincides with pYAP induction, cytosolic location of YAP and a loss of the invasive phenotype (Figure 1 and Supplementary Figure S2A and S2C). Complementary to our observation, Kim et al [51] reported that forced exogenous expression of E-cadherin in MDA-MB-231 cells restored YAP nuclear exclusion in the cells and the authors implicate E-cadherin homophilic interaction as a cell-cell signal that controls YAP activity. Hippo pathway signaling has been shown to contribute to EMT also through the TFGβ-SMAD pathway[47] and cancer cell / stromal crosstalk through secreted factors was shown to modulate EMT [44]. Furthermore, the function of oncogenic drivers of EMT such as KRAS in pancreatic cancer progression is dependent on Hippo pathway signaling for cancer cell as well as the resulting stromal growth and survival signals [24, 48]. Also, Tenascin C (TNC), an extracellular matrix protein,

was reported to support the metastatic seeding of cancer cells and uses stem cell signaling paths that include musashi homolog 1 (MSI1) [49]. Here we found TNC upregulated in the low growth density, invasive MDA-MB-231 cell population (Figure 6A). Beyond these proteins the miR-29b pathway is downregulated upon transcriptional inhibiton of YAP in invasive cells (Supplementary Figure S6A). MiR29b is a suppressor of angiogenesis and metastasis [50], and downmodulation of its pathway will contribute to the induction of the vascular invasive phenotype.

The use of zebrafish in cancer research is attractive due to unique characteristics that include translucent embryos that allow for monitoring of cancer cell behavior in live animals [29, 52]. Here we monitored intravasation of MDA-MB-231 cells from the yolk sac into the circulation as one model system (Figure 2a). We also used Tg(kdrl:GRCFP)zn1 transgenic zebrafish where the green fluorescent endothelia enabled us to visualize and quantify cancer cell extravasation from the circulation into the neighboring tissue (Figure 2c) within 1 or 2 days after cancer cell injection. Also, blockade of CXCR2 (Figure 6d and 6e) revealed the crucial role of this pathway for the extravasation of invasive cancer cells into tissues. We were surprised to find that anti-CXCR2 not only inhibited tissue invasion of cancer cells but induced their re-routing to the fetal hematopoietic organ [35, 36]. From this finding it is tempting to speculate that homing of cancer cells to the bone marrow could be one possible resistance mechanism to cytokine receptor targeting in patients.

Secreted factors contribute to the vascular invasive phenotype and may be amenable to antibody blockade and thus impact the disease course as well as sensitivity or resistance to other treatments. Our data suggest that the invasive phenotype of cancer cells is surprisingly malleable and can be impacted in a reversible manner by changes of cell growth density in culture within a few days (see Fig. S3). It would appear important to take this aspect into account when evaluating drivers of malignant progression or drugs that may interfere with such pathways. It is noteworthy that the invasive phenotype is reversible suggesting that there is no obvious selection of genotypically different subpopulations, a notion that was supported by comparative genomic hybridization (CGH) analysis of DNA from the cell subpopulations grown at high and low densities. Overall, we conclude that altered growth density of cancer cells impacts their vascular invasive phenotype through autocrine and paracrine acting cytokines that signal through CXCR2 and are controlled by LATS1-YAP in the Hippo pathway.

MATERIALS AND METHODS

Cell culture

Primary Human Umbilical Vein Endothelial Cells (HUVECs) were maintained as recommended by the supplier (Lonza, Walkersville, MD). U87, PC3, E0771, parental MDA-MB-231, and MDA-MB-231-derived BrM, BoM, and LM cells were grown in DMEM (GIBCO, Invitrogen) with 10% foetal bovine serum. Low-density cells were propagated at 50-70% confluency, and high-density cells were kept at 100% confluency for 5 days. The inset in Figure 1c shows a phase contrast image from a plate of cells grown at low and high density. Low and high density cells were trysinized and dissociated to a single cell suspension prior to all in vitro and in vivo assay. Complete media were changed daily for

both conditions. For the collection of conditioned media (CM), cells were grown overnight in serum-free DMEM. Collected CM were concentrated 3-fold to 4-fold using vivaspin columns with a cut-off >5 kDa (GE Healthcare). The conditional vascular invasive phenotype was reversible, suggesting that there was no selection of genetically different subpopulations. That notion was supported by comparative genomic hybridization (CGH) analysis of DNA from cells grown at high and low densities, respectively, which included the loci of significantly regulated genes. YAP knockdown cell lines were made using pLKO-shRNA lentiviral construct targeting YAP (Thermo Scientific Open Biosystems) (TRCN0000107266: 5'-TTCTTTATCTAGCTTGGTGGC-3') and (TRCN0000107268: 5-AAAGGATCTGAGCTATTGGTC-3'). LATS1 knockdown cell lines were made using MISSION lentiviral constructs (TRCN0000001779: 5'-CCGGCAAGTCAGAAATCCACCCAAACTCGAGTTTGGGTGGATTTCTGACTTGTTTTT-'3) and (TRCN000000180: 5'-CCGGGAGAAATTAAGCCATCGTGTTCTCGAGAACACGATGGCTTAATTTCTCTTTTT-'3)

Functional screen for pathways that enhance endothelial attachment

MDA-MB-231 cells were transduced with a kinome-wide shRNA library (System Biosciences, Mountain View, CA) and propagated at high density, causing them to lose their invasiveness, and then added to an endothelial monolayer. Puromycin resistance present in kinome-library MDA-MB-231 cells but not in endothelial cells was utilized to collect attached MDA-MB-231 cell clones, which were grown to high density, and subjected to another round of attachment to endothelial cells to enrich for MDA-MB-231 cell clones with enhanced attachment. After the fourth round of selection, shRNAs enriched among the selected clones were identified using Affymetrix hybridization following the manufacturer's protocol (System Biosciences).

Endothelial monolayer invasion assay

HUVECs were plated in the wells of an electric cell-substrate impedance sensing (ECIS) system. The wells had been pretreated with 0.1% gelatine for 30 min and then washed twice with 1× PBS. The cells were grown for approximately 24 h using the 8W10E array 8 instrument (150,000 cells) from Applied Biophysics or the E-plate 33 instrument (30,000 cells) from xCELLigence [53] until a complete monolayer formed with a steady-state impedance reading. Cancer cells (50,000 or 15,000 cells in the 8W10E array 8 and E-plate 33 instruments, respectively) were then added to the monolayers to determine their invasive capacity. Changes in the electric impedance of the monolayer were measured at 5 min intervals. In some experiments, the cancer cells or the endothelial monolayers were pretreated with CM or with antibodies, as indicated in the respective figures.

Endothelial monolayer wound healing assay

Endothelial cells (150,000 cells) were plated in the 8W10E array ECIS system for 24 h until an intact monolayer formed. The wells had been pretreated with 0.1% gelatine for 30 min and then washed twice with 1× PBS. After the formation of an intact monolayer, pulses of high voltage were sent through the electrode array for 5 min to kill the cells growing directly on the electrodes. The impedance dropped by more than 80% until the cells neighbouring

the electrodes repaired the monolayer defect, covering the denuded area on the electrodes and restoring the original level of impedance. The kinetics of the wound closure were monitored in real-time, and the effects of different treatment conditions on the wound closure were compared. The monolayers were treated with CM from cancer cells or CXCR2 antibodies (R&D Systems) 6 h before wounding. This wounding assay relative to the conventional “scratch assay” followed by image analysis were described recently [54, 55].

Cell migration

A two-chamber assay (CIM-plate from xCELLigence; Roche [53]) was used to monitor cancer cell migration. The chambers contained serum-free DMEM with or without IL8 (BD Pharminogen) or anti-CXCR2 (R&D Systems) added to both the upper and lower chamber of the assay system. Cancer cells were grown in serum-free DMEM overnight before harvesting for the assay.

cDNA arrays and data analysis

Analysis of mRNA expression was done by cDNA arrays as described previously [56]. Data were analysed using Bioconductor software. Greater than 2-fold difference in expression and a p-value less than 0.01 were set as the threshold for significance.

Zebrafish injection and imaging

To monitor vascular invasion of cancer cells from the yolk sacs, zebrafish embryos were injected with 100 to 200 MDA-MB-231 cells 48 h post fertilisation (hpf). The injection site is indicated by the syringe in Figure 2a. The injected cells were labelled with 565 nm or 655 nm Q-dots using the Qtracker Cell Labeling kit from Invitrogen.

To monitor extravasation of cancer cells into surrounding tissues, ten to fifty cancer cells labelled with CellTracker™ fluorescent probes from Invitrogen were injected directly into the circulation via the duct of Cuvier (DoC) which opens into the heart of zebrafish embryos. The position of the injection site is indicated in Figure 1e. Tg(kdrl:GRCFP)zn1 zebrafish embryos were injected at 48 hpf (n=24) and monitored by fluorescence microscopy for 24 to 48 h. In some experiments cancer cells were treated with anti-CXCR2 (R&D Systems) or with 1 μM verteporfin (Sigma Aldrich) 6 h prior to injection.

Injections into mice

Studies in mice were reviewed and approved by the Georgetown University Animal Care and Use Committee (GUACUC). Ten thousand E0771 or MDA-MB-231cells were injected into the tail veins of athymic nude mice. After 14 days, the lungs and liver (control organ) were collected, and the total RNA was extracted using an RNeasy Mini Kit (Qiagen) according to the manufacturer's instructions. cDNA was synthesised with the iScript cDNA synthesis kit according to the manufacturer's protocol (Biorad Laboratories, Hercules, CA). qRT-PCR was performed in an iCycler iQ (BioRad) using the iQ SYBR Green Supermix (BioRad) under the following conditions: 95°C for 3 min followed by 40 cycles (95°C for 20 s, 55°C for 30 s, and 72°C for 40 s). The ratio of the mouse actin housekeeping gene to the puromycin resistance gene was used to quantify E0771 cells forming metastases in the lung.

Histology analysis

Hematoxylin and eosin, IHC, and immunofluorescence analyses were performed on paraffin-embedded 5-μm sections using antibodies to YAP (Santa Cruz, Dallas, TX) and PCNA (Sigma-aldrich) and standard protocols described previously [57].

Western blots

Cells were grown at either high or low density in culture and then lysed. Proteins extracted from the lysates were separated by SDS-PAGE and immunoblotted with anti-vimentin (Dako, Carpinteria, CA), beta-catenin (BD Biosciences, San Jose, CA), actin (Millipore, Billerica, MA), E-Cadherin, Stat3, phospho-Stat3, NFκB, phospho-NFκB, IκBα, phospho-IκBα, phospho-YAP (S127) (Cell Signaling, Boston, MA), and YAP (Santa Cruz, Dallas, TX).

Cytokine Array

MDA-MB-231 cells were grown at low density in culture and treated with 1 μM VP for 24 h in serum-free DMEM. Conditioned media was collected and concentrated as described earlier. A RayBio® Human Cytokine Antibody Array 5 (Raybiotech, Norcross, GA) was used according to the manufacture's protocol.

Statistical analysis

Prism 5 (Graphpad Inc) was used for statistical analysis and graphing. ANOVA was used for multiple comparisons and t-tests were used for paired comparisons, with $p<0.05$ as the threshold for statistical significance in all tests. To generate a heat map for the cytokine array, a calibration curve was created using positive and negative controls. The heat map shows the fold change after the data were centred on the mean of the two samples and divided by the standard deviation.

Supplementary Material

Refer to Web version on PubMed Central for supplementary material.

Acknowledgements

Dr. Joan Massague kindly provided the MDA-MB-231 derivative cell lines used here. We thank Caroline E. Laverriere for excellent assistance with the zebrafish experiments. Work was supported by NIH/NCI grant CA71508 (AW) and CA113477 (ATR) and CA51008 for zebrafish and mouse studies.

References

1. Fidler IJ. The pathogenesis of cancer metastasis: the ‘seed and soil’ hypothesis revisited. Nat Rev Cancer. 2003; 3:453–458. [PubMed: 12778135]
2. Nguyen DX, Bos PD, Massagué J. Metastasis: from dissemination to organ-specific colonization. Nat Rev Cancer. 2009; 9:274–284. [PubMed: 19308067]
3. Erez N, Coussens LM. Leukocytes as paracrine regulators of metastasis and determinants of organ-specific colonization. Int J Cancer. 2011; 128:2536–2544. [PubMed: 21387299]
4. Yagi H, Tan W, Dillenburg-Pilla P, Armando S, Amornphimoltham P, Simaan M, et al. A Synthetic Biology Approach Reveals a CXCR4-G13-Rho Signaling Axis Driving Transendothelial Migration of Metastatic Breast Cancer Cells. Science Signaling. 2011; 4:ra60. [PubMed: 21934106]

5. Huh SJ, Liang S, Sharma A, Dong C, Robertson GP. Transiently entrapped circulating tumor cells interact with neutrophils to facilitate lung metastasis development. Cancer Res. 2010; 70:6071–6082. [PubMed: 20610626]
6. Friedl P, Locker J, Sahai E, Segall JE. Classifying collective cancer cell invasion. Nat Cell Biol. 2012; 14:777–783. [PubMed: 22854810]
7. Hanahan D, Weinberg RA. The hallmarks of cancer. Cell. 2000; 100:57–70. [PubMed: 10647931]
8. Zeng Q, Hong W. The emerging role of the hippo pathway in cell contact inhibition, organ size control, and cancer development in mammals. Cancer Cell. 2008; 13:188–192. [PubMed: 18328423]
9. Tao W, Zhang S, Turenchalk GS, Stewart RA, St John MA, Chen W, et al. Human homologue of the Drosophila melanogaster lats tumour suppressor modulates CDC2 activity. Nature genetics. 1999; 21:177–181. [PubMed: 9988268]
10. St John MA, Tao W, Fei X, Fukumoto R, Carcangiu ML, Brownstein DG, et al. Mice deficient of Lats1 develop soft-tissue sarcomas, ovarian tumours and pituitary dysfunction. Nature genetics. 1999; 21:182–186. [PubMed: 9988269]
11. Pan D. The hippo signaling pathway in development and cancer. Dev Cell. 2010; 19:491–505. [PubMed: 20951342]
12. Harvey KF, Zhang X, Thomas DM. The Hippo pathway and human cancer. Nat Rev Cancer. 2013; 13:246–257. [PubMed: 23467301]
13. Mo J-S, Park HW, Guan K-L. The Hippo signaling pathway in stem cell biology and cancer. EMBO reports. 2014; 15:642–656. [PubMed: 24825474]
14. Varelas X. The Hippo pathway effectors TAZ and YAP in development, homeostasis and disease. Development. 2014; 141:1614–1626. [PubMed: 24715453]
15. Nance J. Cell biology in development: Getting to know your neighbor: Cell polarization in early embryos. The Journal of Cell Biology. 2014; 206:823–832. [PubMed: 25267293]
16. Dong J, Feldmann G, Huang J, Wu S, Zhang N, Comerford SA, et al. Elucidation of a universal size-control mechanism in Drosophila and mammals. Cell. 2007; 130:1120–1133. [PubMed: 17889654]
17. Piccolo S, Dupont S, Cordenonsi M. The Biology of YAP/TAZ: Hippo Signaling and Beyond. Physiol Rev. 2014; 94:1287–1312. [PubMed: 25287865]
18. Egeblad M, Nakasone ES, Werb Z. Tumors as organs: complex tissues that interface with the entire organism. Developmental Cell. 2010; 18:884–901. [PubMed: 20627072]
19. Park HW, Guan K-L. Regulation of the Hippo pathway and implications for anticancer drug development. Trends in Pharmacol Sci. 2013; 34:581–589. [PubMed: 24051213]
20. Chen Q, Zhang N, Gray RS, Li H, Ewald AJ, Zahnow CA, et al. A temporal requirement for Hippo signaling in mammary gland differentiation, growth, and tumorigenesis. Genes & Development. 2014; 28:432–437. [PubMed: 24589775]
21. Lamar JM, Stern P, Liu H, Schindler JW, Jiang Z-G, Hynes RO. The Hippo pathway target, YAP, promotes metastasis through its TEAD- interaction domain. Proc Natl Acad Sci USA. 2012; 109:E2441–2450. [PubMed: 22891335]
22. Nallet-Staub F, Marsaud V, Li L, Gilbert C, Dodier S, Bataille V, et al. Pro invasive activity of the Hippo pathway effectors YAP and TAZ in cutaneous melanoma. J Invest Dermatol. 2014; 134:123–132. [PubMed: 23897276]
23. Lau AN, Curtis SJ, Fillmore CM, Rowbotham SP, Mohseni M, Wagner DE, et al. Tumor-propagating cells and Yap/Taz activity contribute to lung tumor progression and metastasis. EMBO J. 2014; 33:468–481. [PubMed: 24497554]
24. Zhang W, Nandakumar N, Shi Y, Manzano M, Smith A, Graham G, et al. Downstream of Mutant KRAS, the Transcription Regulator YAP Is Essential for Neoplastic Progression to Pancreatic Ductal Adenocarcinoma. Science Signaling. 2014; 7:ra42. [PubMed: 24803537]
25. Greten FR. YAP1 Takes Over when Oncogenic K-Ras Slumbers. Cell. 2014; 158:11–12. [PubMed: 24995973]
26. Bos PD, Zhang XH-F, Nadal C, Shu W, Gomis RR, Nguyen DX, et al. Genes that mediate breast cancer metastasis to the brain. Nature. 2009; 459:1005–1009. [PubMed: 19421193]

27. Kang Y, Siegel PM, Shu W, Drobnjak M, Kakonen SM, Cordón-Cardo C, et al. A multigenic program mediating breast cancer metastasis to bone. Cancer Cell. 2003; 3:537–549. [PubMed: 12842083]
28. Minn AJ, Gupta GP, Siegel PM, Bos PD, Shu W, Giri DD, et al. Genes that mediate breast cancer metastasis to lung. Nature. 2005; 436:518–524. [PubMed: 16049480]
29. Stoletov K, Kato H, Zardouzian E, Kelber J, Yang J, Shattil S, et al. Visualizing extravasation dynamics of metastatic tumor cells. J Cell Sci. 2010; 123:2332–2341. [PubMed: 20530574]
30. Cross LM, Cook MA, Lin S, Chen J-N, Rubinstein AL. Rapid analysis of angiogenesis drugs in a live fluorescent zebrafish assay. Arterioscler Thromb Vasc Biol. 2003; 23:911–912. [PubMed: 12740225]
31. Liu-Chittenden Y, Huang B, Shim JS, Chen Q, Lee S-J, Anders RA, et al. Genetic and pharmacological disruption of the TEAD-YAP complex suppresses the oncogenic activity of YAP. Genes & Development. 2012; 26:1300–1305. [PubMed: 22677547]
32. Ishimoto T, Nagano O, Yae T, Tamada M, Motohara T, Oshima H, et al. CD44 variant regulates redox status in cancer cells by stabilizing the xCT subunit of system xc(−) and thereby promotes tumor growth. Cancer Cell. 2011; 19:387–400. [PubMed: 21397861]
33. Liu C, Kelnar K, Liu B, Chen X, Calhoun-Davis T, Li H, et al. The microRNA miR-34a inhibits prostate cancer stem cells and metastasis by directly repressing CD44. Nat Med. 2011; 17:211–215. [PubMed: 21240262]
34. O'Connell JT, Sugimoto H, Cooke VG, Macdonald BA, Mehta AI, Lebleu VS, et al. VEGF-A and Tenascin-C produced by S100A4+ stromal cells are important for metastatic colonization. Proc Natl Acad Sci USA. 2011; 108:16002–16007. [PubMed: 21911392]
35. Oehlers SHB, Flores MV, Hall CJ, O'Toole R, Swift S, Crosier KE, et al. Expression of zebrafish cxcl8 (interleukin-8) and its receptors during development and in response to immune stimulation. Dev Comp Immunol. 2010; 34:352–359. [PubMed: 19941893]
36. van der Aa LM, Chadzinska M, Tijhaar E, Boudinot P, Verburg-van Kemenade BML. CXCL8 chemokines in teleost fish: two lineages with distinct expression profiles during early phases of inflammation. PLoS ONE. 2010; 5:e12384. [PubMed: 20865040]
37. Hanahan D, Weinberg RA. Hallmarks of cancer: the next generation. Cell. 2011; 144:646–674. [PubMed: 21376230]
38. Chen D, Sun Y, Wei Y, Zhang P, Rezaeian AH, Teruya-Feldstein J, et al. LIFR is a breast cancer metastasis suppressor upstream of the Hippo-YAP pathway and a prognostic marker. Nat Med. 2012; 18:1511–1517. [PubMed: 23001183]
39. Iorns E, Ward TM, Dean S, Jegg A, Thomas D, Murugaesu N, et al. Whole genome in vivo RNAi screening identifies the leukemia inhibitory factor receptor as a novel breast tumor suppressor. Breast Cancer Res Treat. 2012; 135:79–91. [PubMed: 22535017]
40. Bieche I, Chavey C, Andrieu C, Busson M, Vacher S, Le Corre L, et al. CXC chemokines located in the 4q21 region are up-regulated in breast cancer. Endocr Relat Cancer. 2007; 14:1039–1052. [PubMed: 18045955]
41. Acharyya S, Oskarsson T, Vanharanta S, Malladi S, Kim J, Morris PG, et al. A CXCL1 Paracrine Network Links Cancer Chemoresistance and Metastasis. Cell. 2012; 150:165–178. [PubMed: 22770218]
42. Korkaya H, Kim G-I, Davis A, Malik F, Henry NL, Ithimakin S, et al. Activation of an IL6 inflammatory loop mediates trastuzumab resistance in HER2+ breast cancer by expanding the cancer stem cell population. Mol Cell. 2012; 47:570–584. [PubMed: 22819326]
43. Yang L, Huang J, Ren X, Gorska AE, Chytil A, Aakre M, et al. Abrogation of TGF beta signaling in mammary carcinomas recruits Gr-1+CD11b+ myeloid cells that promote metastasis. Cancer Cell. 2008; 13:23–35. [PubMed: 18167337]
44. Rasanen K, Herlyn M. Paracrine Signaling between Carcinoma Cells and Mesenchymal Stem Cells Generates Cancer Stem Cell Niche via Epithelial- Mesenchymal Transition. Cancer Discov. 2012; 2:775–777. [PubMed: 22969117]
45. Kim MY, Oskarsson T, Acharyya S, Nguyen DX, Zhang XH-F, Norton L, et al. Tumor self-seeding by circulating cancer cells. Cell. 2009; 139:1315–1326. [PubMed: 20064377]

46. Fernando RI, Castillo MD, Litzinger M, Hamilton DH, Palena C. IL-8 signaling plays a critical role in the epithelial-mesenchymal transition of human carcinoma cells. Cancer Res. 2011; 71:5296–5306. [PubMed: 21653678]
47. Varelas X, Samavarchi-Tehrani P, Narimatsu M, Weiss A, Cockburn K, Larsen BG, et al. The Crumbs complex couples cell density sensing to Hippo-dependent control of the TGF-β-SMAD pathway. Dev Cell. 2010; 19:831–844. [PubMed: 21145499]
48. Shao DD, Xue W, Krall EB, Bhutkar A, Piccioni F, Wang X, et al. KRAS and YAP1 Converge to Regulate EMT and Tumor Survival. Cell. 2014; 158:171–184. [PubMed: 24954536]
49. Oskarsson T, Acharyya S, Zhang XH-F, Vanharanta S, Tavazoie SF, Morris PG, et al. Breast cancer cells produce tenascin C as a metastatic niche component to colonize the lungs. Nat Med. 2011; 17:867–874. [PubMed: 21706029]
50. Melo SA, Kalluri R. miR-29b moulds the tumour microenvironment to repress metastasis. Nat Cell Biol. 2013; 15:139–140. [PubMed: 23377028]
51. Kim N-G, Koh E, Chen X, Gumbiner BM. E-cadherin mediates contact inhibition of proliferation through Hippo signaling-pathway components. Proc Natl Acad Sci USA. 2011; 108:11930–11935. [PubMed: 21730131]
52. Stoletov K, Klemke R. Catch of the day: zebrafish as a human cancer model. Oncogene. 2008; 27:4509–4520. [PubMed: 18372910]
53. Abassi YA, Xi B, Zhang W, Ye P, Kirstein SL, Gaylord MR, et al. Kinetic cell-based morphological screening: prediction of mechanism of compound action and off-target effects. Chemistry & Biology. 2009; 16:712–723. [PubMed: 19635408]
54. Al-Otaiby M, Tassi E, Schmidt MO, Chien CD, Baker T, Salas AG, et al. Role of the Nuclear Receptor Coactivator AIB1/SRC-3 in Angiogenesis and Wound Healing. The American Journal of Pathology. 2012; 180:1474–1484. [PubMed: 22342158]
55. Tassi E, Mcdonnell K, Gibby KA, Tilan JU, Kim SE, Kodack DP, et al. Impact of fibroblast growth factor-binding protein-1 expression on angiogenesis and wound healing. The American Journal of Pathology. 2011; 179:2220–2232. [PubMed: 21945411]
56. Oh A, List H-J, Reiter R, Mani A, Zhang Y, Gehan E, et al. The nuclear receptor coactivator AIB1 mediates insulin-like growth factor I-induced phenotypic changes in human breast cancer cells. Cancer Res. 2004; 64:8299–8308. [PubMed: 15548698]
57. Fereshteh MP, Tilli MT, Kim SE, Xu J, O'Malley BW, Wellstein A, et al. The nuclear receptor coactivator amplified in breast cancer-1 is required for Neu (ErbB2/HER2) activation, signaling, and mammary tumorigenesis in mice. Cancer Res. 2008; 68:3697–3706. [PubMed: 18483252]

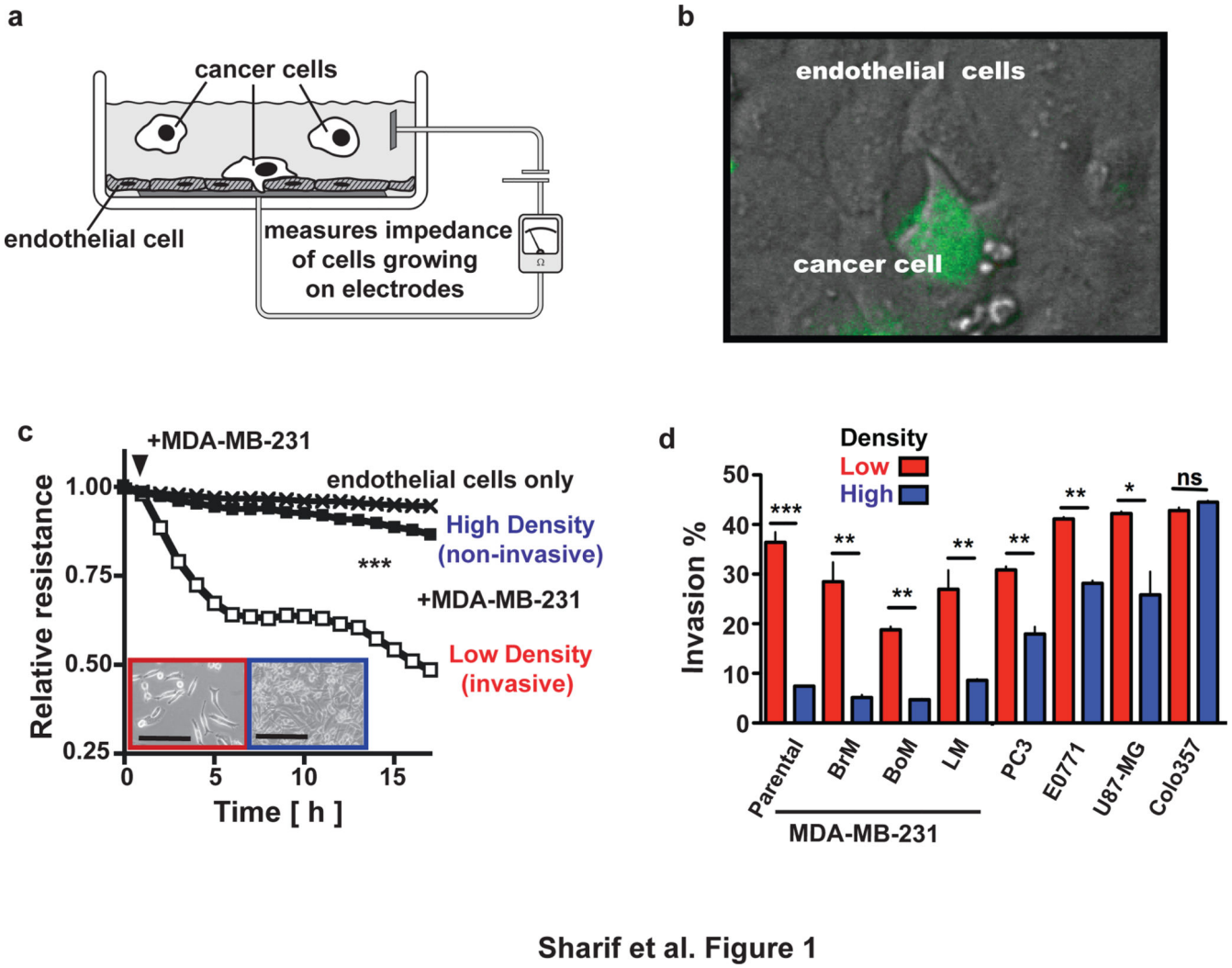

Figure 1.

The endothelial monolayer invasive capacity of cancer cells is affected by their growth density. (**a**) Schematic of a cancer cell invasion assay into an endothelial monolayer. Electric Cell-substrate Impedance Sensing (ECIS) provides a readout of monolayer disruption. (**b**) Image of a cancer cell (green; labeled with fluorescent dye) invading an endothelial monolayer. (**c**) ECIS real-time readout of endothelial monolayers after the addition of MDA-MB-231 cells grown previously at low or high density (inset; size bar = 0.1 mm); *** $p<0.0001$, low vs. high. (**d**)Percentage of invasion by different cancer cell lines propagated at low or high density. The reading was taken 10 h after addition of cancer cells. BoM, LM, and BrM are MDA-MB-231 derivative lines that preferentially metastasize to the brain, bone or lung [26–28]. ** $p<0.001$; *** $p<0.0001$; ns, not significant.

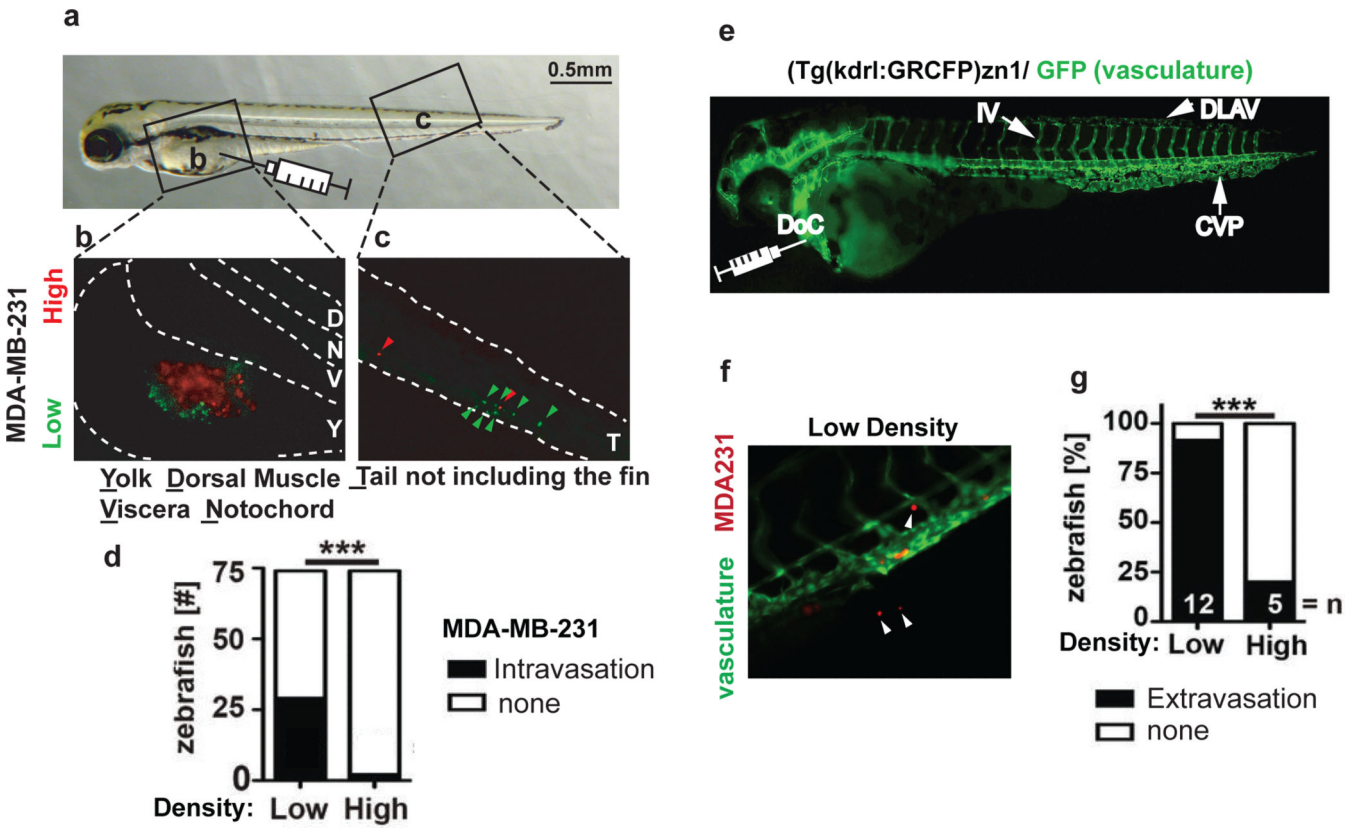

Figure 2.

Cell growth density in vitro affects intravasation and extravasation.(**a**) Representative image of a zebrafish embryo 4 d after fertilization. The boxed areas mark the yolk sac (**b**) and tail region (**c**) shown as fluorescent images in panels b & c. The syringe indicates the location of injection of labeled tumor cells into the yolk sac from where the tumor cells intravasate. (**b,c**) Representative fluorescent images of the yolk sac (**b**) and tail (**c**) regions of a zebrafish embryo whose yolk sac was injected simultaneously with MDA-MB-231 cells grown at low or high density and labelled with green or red dyes. Dotted lines mark the boundaries of the yolk sac (**b**) and the tail region (**c**). Red arrowheads indicate high density cells and green arrowheads indicate low density cells that invaded the vasculature to reach the tail region. (**d**) The number of zebrafish embryos with or without detectable intravasated MDA-MB-231 cells in the tail region 2 d after injection. *** $p<0.0001$. (**e**) Fluorescent image of a (kdrl:GRCFP)zn1 zebrafish with green fluorescent vasculature 4 d after fertilization. DLAV, Dorsal Longitudinal Anastomotic Vessel; IV, Intersegmental Vessel; CVP, Caudal Vein Plexus; DoC, duct of Cuvier. The syringe points to the site for direct intravascular injection of labeled tumor cells. (**f**) Representative image of the tail of a (kdrl:GRCFP)zn1 zebrafish after intravascular injection with red-labelled MDA-MB-231 cells. White arrowheads indicate cells extravasated from the green fluorescent vasculature. (**g**) Percentage of kdrl:GRCFP)zn1 zebrafish embryos containing MDA-MB-231 cells extravasated into neighboring tissues 2 d after intravascular injections. n, number of fish analyzed; *** $p<0.0001$.

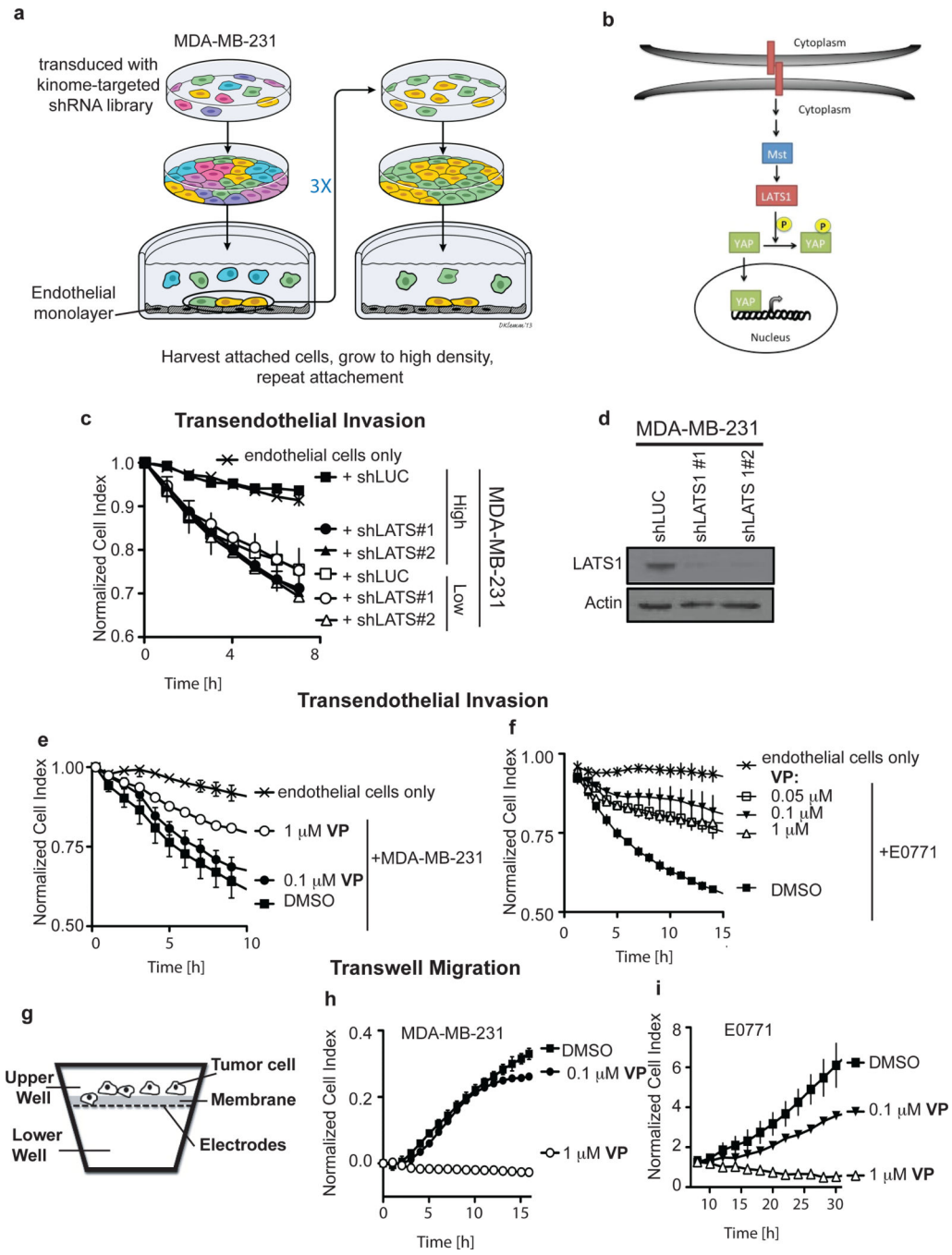

Figure 3.

LATS1-YAP signaling controls cancer cell invasiveness in vitro. (**a**) Schematic of the functional screen for drivers of endothelial monolayer invasion. Cancer cells were transduced with a kinome-wide shRNA library and grown to high density to render the population non-invasive. Over three rounds cells were selected for endothelial attachment and invasion. (**b**) Schematic of the Hippo pathway in which LATS1 phosphorylates and inhibits YAP function. (**c**) Transendothelial invasion of low and high density cells with LATS1 knocked down. (**d**) LATS1 western blot of MDA-MB-231 cells infected with shLuc

or shLATS1. Actin was used as a loading control. (**e, f**) The effect of verteporfin (VP), a YAP activity inhibitor, on MDA-MB-231 and E0771 cells invading an endothelial monolayer in the ECIS assay (see Figure 1a). (**g**) Schematic of a transwell Boyden-chamber assay to monitor cell migration. The chambers are separated by a porous membrane carrying an electrode array facing the lower chamber. Cells are added to the top chamber, and migrating cells are detected by ECIS. (**h, i**) The effect of VP on transwell migration by MDA-MB-231 and E0771 cells.

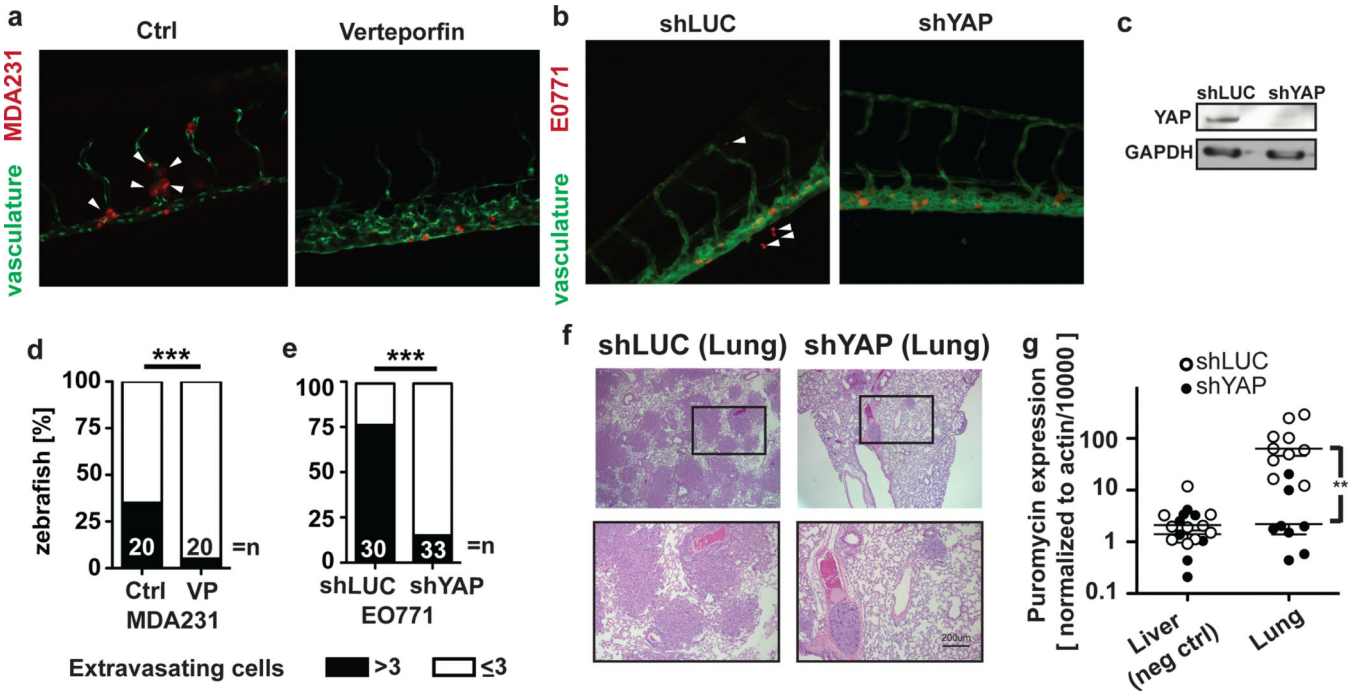

Figure 4.

YAP activity impacts cancer cells vascular invasion and metastasis. (**a, b**) Representative images of the tail vasculature of kdrl:GRCFP zebrafish embryos injected with low density MDA-MB-231 cells treated with vehicle or verteporfin (VP) and E0771 cells infected with control (shLUC) or YAP shRNAs (shYAP) and selected for puromycin resistance. (**c**) YAP Western blot of E0771 cells infected with shLuc or shYAP. GAPDH was used as a loading control. (**d, e**) Quantitation of extravasated MDA-MB-231 and E0771 cells from **(a)** and (**b**) 2 d after intravascular injection into kdrl:GRCFP zebrafish; *** $p<0.0001$. (**f**) H&E staining of mouse lung sections after tail vein injection of E0771 cells expressing either shLUC or shYAP. (**g**) Quantitation of metastases in lung tissues by qRT-PCR analysis for puromycin expression. Liver tissues served as a negative control. ** $p<0.001$.

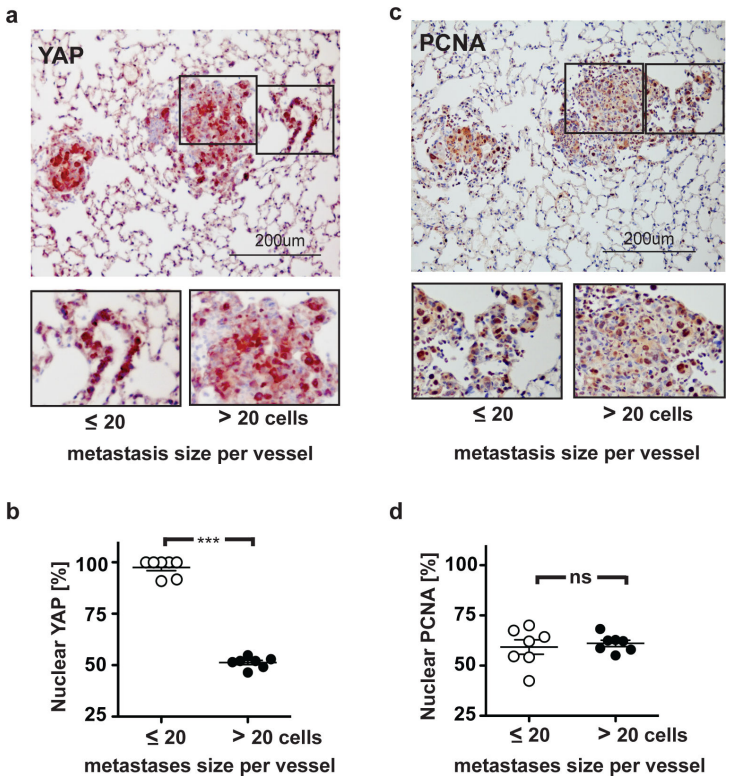

Figure 5.

YAP protein cellular location in lung metastases after extravasation and metastatic growth. (**a**) Immunohistochemistry (IHC) for YAP protein in lung sections with E0771 cell metastases containing shLUC. (**b**) Percent of cells with nuclear YAP protein in metastases after extravasation (small; < 20 cells) and further growth (large; > 20 cells). *** p<0.0001. (**c**) IHC for PCNA in lung sections with E0771 cells containing shLUC. (**d**) Percent of cells with PCNA-positive staining in small and large metastases; ns, not significant.

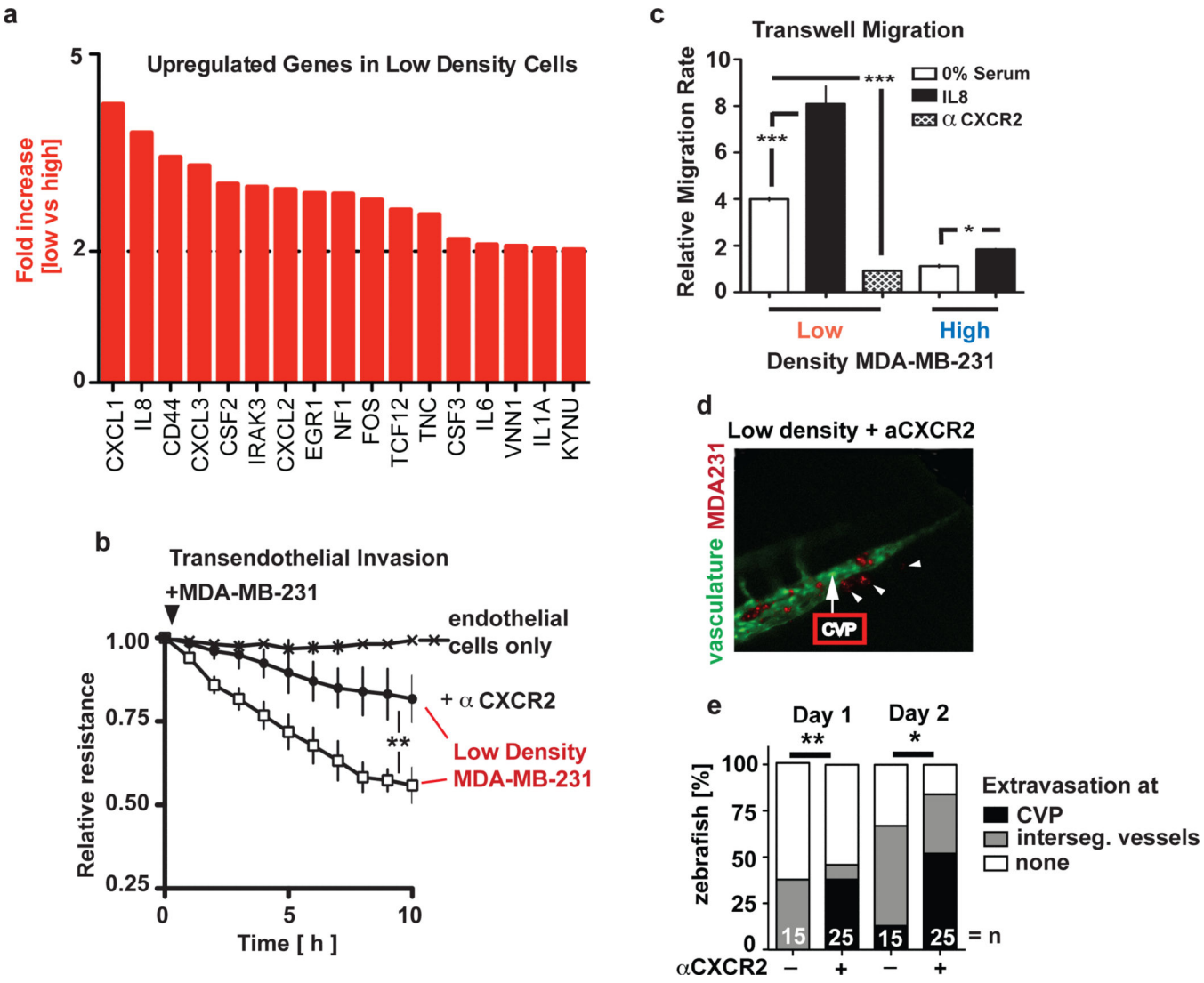

Figure 6.

Cytokines are rate-limiting for the vascular invasive phenotype in vitro and in vivo. (**a**) cDNA array analysis showing up-regulated cytokine genes in MDA-MB-231 cells grown at low versus high density. (**b**) Effect of anti-CXCR2 antibodies on the endothelial invasiveness of MDA-MB-231 cells grown at low density. Note: IL8 and CXCL1, 2, and 3 are ligands for CXCR2. ** $p<0.001$. (**c**) Transwell migration rates of low or high density MDA-MB-231 cells in the absence or presence of IL8 or anti-CXCR2 antibodies. *** $p<0.0001$, * $p<0.01$. (**d**) Representative images of the caudal vein plexus area 2 d after intravascular injection of low density, red labelled MDA-MB-231 cells treated with anti-CXCR2 antibodies. A control image is shown in Figure 2f. (**e**) Percentage of extravasation into tissues from intersegment vessels and at the caudal vein plexus (CVP) of MDA-MB-231 cells from (**d**). n, number of fish analyzed. * $p<0.01$, ** $p<0.001$.

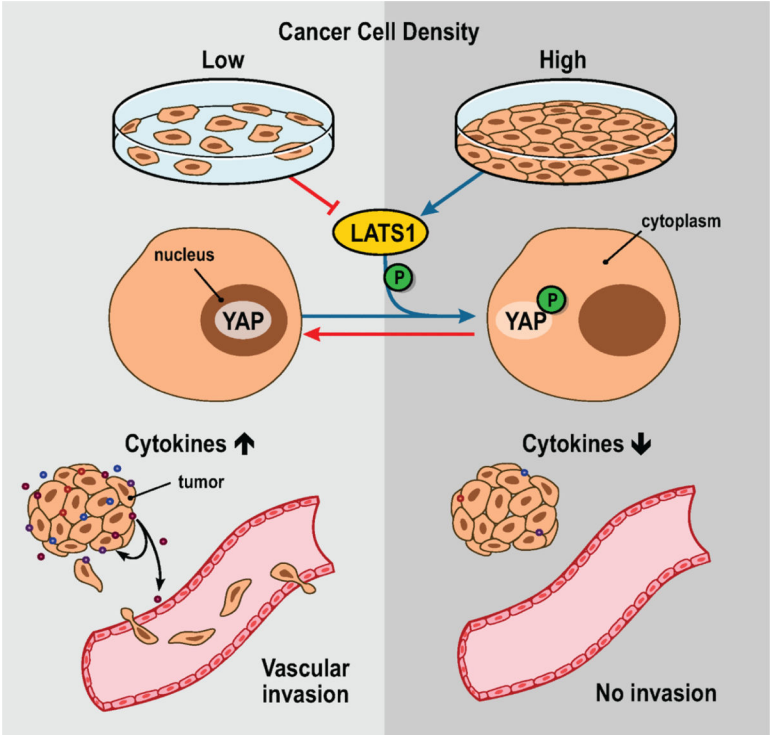

Figure 7.

Graphical abstract of the findings. Altered cancer cell growth density signals via LATS1-YAP to impact the expression of autocrine and paracrine acting cytokines that modulate vascular invasion of cancer cells.